Binding Affinity Prediction of Novel Estrogen Receptor Ligands Using Receptor-Based 3-D QSAR Methods

Wolfgang Sippl*

Institute for Pharmaceutical Chemistry, Heinrich-Heine-Universität Düsseldorf, Universitätsstr. 1, D-40225 Düsseldorf, Germany

Abstract—We have recently reported the development of a 3-D QSAR model for estrogen receptor ligands showing a significant correlation between calculated molecular interaction fields and experimentally measured binding affinity. The ligand alignment obtained from docking simulations was taken as basis for a comparative field analysis applying the GRID/GOLPE program. Using the interaction field derived with a water probe and applying the smart region definition (SRD) variable selection procedure, a significant and robust model was obtained ($q^2_{LOO} = 0.921$, SDEP = 0.345). To further analyze the robustness and the predictivity of the established model several recently developed estrogen receptor ligands were selected as external test set. An excellent agreement between predicted and experimental binding data was obtained indicated by an external SDEP of 0.531. Two other traditionally used prediction techniques were applied in order to check the performance of the receptor-based 3-D QSAR procedure. The interaction energies calculated on the basis of receptor–ligand complexes were correlated with experimentally observed affinities. Also ligand-based 3-D QSAR models were generated using program FlexS. The interaction energy-based model, as well as the ligand-based 3-D QSAR models yielded models with lower predictivity. The comparison with the interaction energy-based model and with the ligand-based 3-D QSAR models, respectively, indicates that the combination of receptor-based and 3-D QSAR methods is able to improve the quality of prediction.
© 2002 Elsevier Science Ltd. All rights reserved.

Introduction

The effect of estrogens is mediated by an intracellular estrogen receptor (ER), which belongs to the steroid/thyroid nuclear hormone superfamily. These receptors act as transcriptional activators via a direct interaction with DNA sequences termed as response elements.[1] The biological action of estradiol, the most active endogenous estrogen, and other ER ligands and their primary interactions with the receptor protein have been topics of much interest over the years.[2–6] Particularly elucidation of the structural requirements, which enable binding of estrogens to the receptor, has actively been pursued as a means to develop novel therapeutic agents. ER ligands are used in a number of clinical applications such as, for example, breast cancer therapy, treatment and prevention of osteoporosis, and in estrogen replacement therapy of postmenopausal women.[2]

In 1997, the crystal structure of the ligand-binding domain of ERα, complexed with estradiol and the nonsteroidal

ligand diethylstilbestrol was reported.[7] Like other members of the nuclear hormone receptor superfamily, the ligand-binding domain of ER has the canonical anti-parallel α-helical triple sandwich topology, with estradiol being completely engulfed within the lower portion of the domain. ER binds a remarkably wide range of steroidal and nonsteroidal compounds, ranging from the classical steroids up to simple phenolic compounds.[4] Recently several new interesting structures for ER ligands have been published.[8–12] Given the diverse range of molecules that may bind to the receptor and exert an effect, there is a considerable interest in developing computational techniques to correctly predict the affinity of novel compounds.

The prediction of novel compounds on the basis of previously synthesized ones is one of the major challenges in today's drug design. The strategies that can be applied for this purpose fall into two major categories—the indirect ligand-based and the direct receptor-based approach. The ligand-based methods, including traditional quantitative structure–activity relationships (QSARs)[13,14] and modern 3-D QSAR techniques such as the comparative molecular field analysis (CoMFA),[15,16]

*Tel.: +49-211-811-3848; fax: +49-211-811-3847; e-mail: sippl@pharm.uni-duesseldorf.de

are based entirely on experimental structure–activity relationships for enzyme inhibitor or receptor ligands. For the direct receptor-based methods, which include molecular docking, molecular dynamics simulation or free energy perturbation methods, the 3-D structure of a target enzyme or even a receptor–effector complex is required with atomic resolution.[17]

3-D QSAR methods, especially CoMFA, are nowadays used widely in drug design, since they are computationally not demanding and afford fast generation of QSARs from which biological activity of newly synthesized molecules can be predicted. If correlated with biological activity, 3-D-fields can be generated, which describe the contribution of a region of interest surrounding the ligands to the target properties. However there is a main difficulty in the application of 3-D QSAR methods such as CoMFA. For a correct model, a spatial orientation of the ligands towards one another has to be found, which is representative for the relative differences in the binding geometry at the protein-binding site. The success of a molecular field analysis is therefore completely determined by the quality of the choice of the superimposition of the studied molecules.[18–21]

On the other hand, structure-based methods are able to calculate fairly accurately the position and orientation of a potential ligand in a receptor binding site. This has been demonstrated by various docking studies, described in the literature.[22–25] Most of the docking programs use empirical potential energy functions to calculate the binding energies of protein–ligand complexes. These functions sum up several basic energy terms, such as Van-der-Waals and Coulomb electrostatic interaction. The major problem of modern docking programs is the inability to evaluate binding free energies correctly in order to rank different ligand–receptor complexes. The problem of predicting affinity has generated considerable interest in developing methods to calculate ligand affinity reliably for a widely diverse series of molecules binding to the same target protein of known structure.[26–30] The main problem in affinity prediction is that the underlying molecular interactions are highly complex and various terms should be taken into account to quantify the free energy of the interaction process. Only rigorous methods, such as free energy perturbation or thermodynamic integration[31] are able to correctly predict binding affinity. While these two methods clearly have the potential of providing accurate evaluation of relative binding free energies, they are very expensive in a computational sense.

Recently, several studies have been published in which the combination of receptor-based methods and 3-D QSAR was successfully applied for the design and prediction of bioactive compounds.[32–36] The three-dimensional structure of a target protein, along with a docking protocol is used to guide alignment selection for comparative molecular field analysis. It is quite appealing to combine the accuracy of a receptor-based alignment with the computational efficiency of a ligand-based method.

Receptor structures, either experimentally resolved or obtained by homology modeling, can provide important information that is critical for an alignment in CoMFA, while QSAR can provide better prediction of binding energies.[36,37]

We applied this receptor-based 3-D QSAR technique on a set of 30 ER agonists including steroidal and non-steroidal compounds.[38,39] The crystal structure of the ligand-binding domain of the ER together with an automatic docking program was used to determine the molecular alignment of the ligands. The 3-D QSAR model, which was obtained from the receptor-based alignment yielded a high correlation between the experimentally determined binding affinity and the calculated molecular interaction fields. We were able to show that the receptor-based 3-D QSAR yields a better prediction of the binding affinity than using an interaction energy-based model or a purely ligand-based 3-D QSAR analysis. Encouraged by these results the receptor-based 3-D QSAR model should now be used for the screening and prediction of new ligands. In the present analysis this approach is applied in order to predict the binding affinity of recently developed ER ligands.

In addition, the binding affinity of these novel ER ligands is estimated on the basis of two further prediction methods. The performance of these methods will be discussed and compared with the results obtained using the receptor-based 3-D QSAR model.
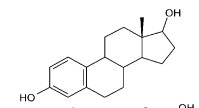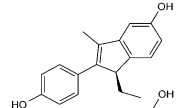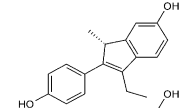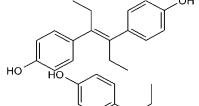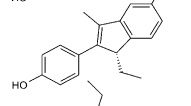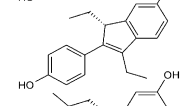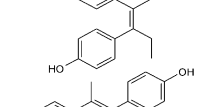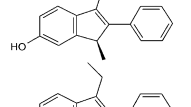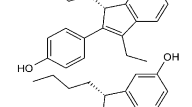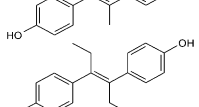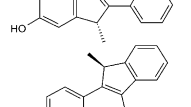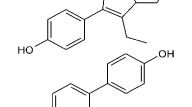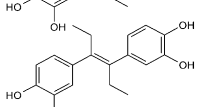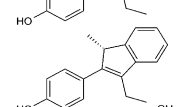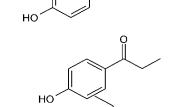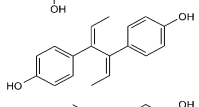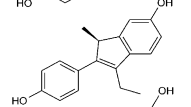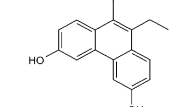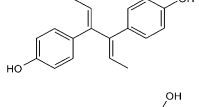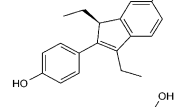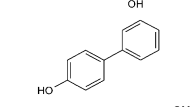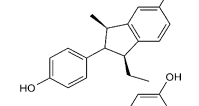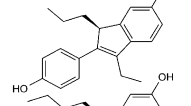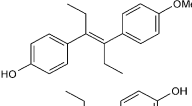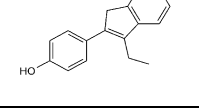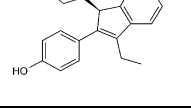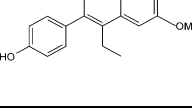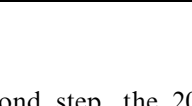
Computational Methods

For the original investigation structure–activity data for a series of 30 structurally diverse ER agonists originally reported by Sadler et al. were selected.[38] The molecular structures of the 30 compounds are displayed in Table 1. The biological activities were expressed as relative binding affinities (RBA) relative to estradiol, which is set to 100. These numbers were then transformed to the decadic log values of the RBA (Table 2). These data were used to develop several 3-D QSAR models in order to predict the binding affinities of new ER ligands. For this purpose, four different test sets of recently developed ER ligands were selected.[8,10,11] The molecular structures together with the RBA are shown in Tables 2–5. The numbering of the compounds was taken from the original publications

Crystal structures

In 1997, the 3-D structure of the ER alpha isoform has been resolved by Brzozowski et al.[7] To model the receptor–ligand complexes, the coordinates of the human ER alpha isoform ligand-binding domain liganded with estradiol and diethylstilbestrol were taken from the Protein Databank.[40] Polar hydrogen atoms were added, charges from AMBER[41] were loaded, and the whole molecule was subjected to a minimization using the AMBER force field[42,43] keeping all protein backbone atoms at fixed positions.

W. Sippl / Bioorg. Med. Chem. 10 (2002) 3741–3755

3743

Table 1. Structure of 30 estrogen receptor ligands used for the generation of the receptor-based 3-D QSAR model

Compd.	Structure	Compd.	Structure	Compd.	Structure
c1		c11		c21	
c2		c12		c22	
c3		c13		c23	
c4		c14		c24	
c5		c15		c25	
c6		c16		c26	
c7		c17		c27	
c8		c18		c28	
c9		c19		c29	
c10		c20		c30	

Docking simulations

The docking analysis was performed using a two-stage docking procedure applying the program AutoDock (version 3.0), which has been shown to successfully reproduce experimentally observed binding modes.[44,45] The program is described in detail elsewhere.[23] AutoDock uses a Lamarckian genetic algorithm to explore the binding possibilities of a ligand in a binding pocket. The interaction energy of ligand and protein is evaluated using atom affinity potentials calculated on a grid similar to that described by Goodford.[46] The minimized ligand-free protein structures, as described above, were used as input structure for the docking simulations. All ligand atoms but no protein atoms were allowed to move during the docking simulation. For each ligand the simulation was composed of 100 docking runs using the standard AutoDock parameters. The 100 resulting complexes were clustered with a RMSD tolerance of 0.7 Å.

In the second step low-energy complexes were reranked according to the interaction energy calculated with a more detailed energetic model based on the classical YETI force field.[43,47,48] For this second step, the 20 complexes of the AutoDock energy ranking were selected. The protein structure was held fixed during the minimization, whereas the ligand was allowed to change its conformation and position in the binding pocket. Applying this minimization the ligand conformation is relaxed into a neighboring local energy minimum.

3-D QSAR analysis

The GRID/GOLPE[49,50] method, which is comparable to the traditional CoMFA method, was used within this study to perform 3-D QSAR analysis.[51] For the training set of 30 compounds, three different alignment strategies were examined. One alignment comes directly from the top-scoring YETI orientation and the other two rely on atom-based alignments, which were obtained using program FlexS.[30,52] In FlexS physicochemical properties of molecules to be superimposed are approximated as density distributions in space in terms of associated Gaussian functions. These functions are used to automatically superimpose a flexible molecule onto a rigid template molecule. Two different molecular alignments (alignment A and B) were generated using FlexS.
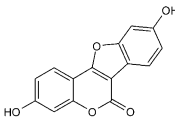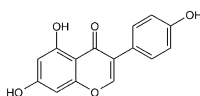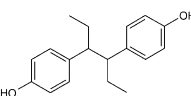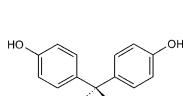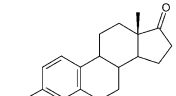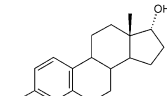
Table 2. Actual and calculated affinities

Compd	logRBA$_{exp}$	logRBA$_{pred}$
c1	2.00	1.99
c2	2.46	2.44
c3	−0.10	0.01
c4	1.52	1.44
c5	2.00	1.98
c6	1.40	1.39
c7	−0.52	−0.60
c8	1.30	1.40
c9	0.30	0.36
c10	1.14	1.07
c11	2.00	2.01
c12	2.15	2.36
c13	0.26	0.17
c14	−0.70	−0.54
c15	0.75	0.68
c16	−0.05	0.01
c17	2.46	2.36
c18	2.47	2.51
c19	2.36	2.33
c20	2.25	2.32
c21	1.11	0.93
c22	1.04	1.03
c23	1.26	1.26
c24	0.90	0.95
c25	−1.70	−1.76
c26	−1.00	−0.96
c27	−0.80	−0.80
c28	−1.70	−1.67
c29	1.30	1.29
c30	1.00	0.94

Alignment A was obtained by superimposing the remaining 29 compounds on diethylstilbestrol, whereas alignment B was obtained by taking estradiol as template molecule for the fitting process.

For each alignment, the interaction field between the ligands and a water probe was calculated using the GRID program employing a grid spacing of 1 Å. The size of the grid box used for the calculation was defined

Table 3. Observed and predicted estrogen receptor binding affinity (RBA) of the six compounds of test set 1

Coumestrol　　　Genistein　　　Hexestrol

Bisphenol A　　　Estrone　　　17 α-Estradiol

Compd	logRBA$_{exp}$
Coumestrol	1.97
Genistein	0.70
Hexestrol	2.25
Bisphenol A	−1.30
Estrone	1.78
17a-Estradiol	1.76
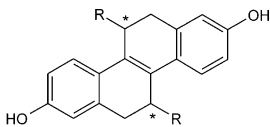
in such a way that it extended approximately 4 Å beyond each of the molecules in each dimension (18×22×19 Å). A cutoff of +5 kcal/mol was applied in order to obtain a more symmetrical distribution between negative and positive interaction energy values which are considered for the statistical analysis[39] (i.e., the GRID interaction energy values which were used for the PLS analysis lie in the range between +5 and −5 kcal/mol). The GRID calculation gave 8740 variables for each compound. A major part of these variables is not important for describing the interaction between the ligand and the receptor and is introducing only noise in the statistical PLS analysis.[53] These variables were selected and eliminated applying the advanced pretreatment procedure and the Smart Region Definition/Fractional Factorial Design (SRD/FFD) variable selection within the GOLPE program (for a detailed description of this approach, see refs 53—55). Models obtained applying variable selection are in general of higher quality than models calculated without variable selection (for example, see refs 36, 39, 53, 55). The GOLPE advanced pretreatment eliminated those variables with absolute values smaller than 0.1 kcal/mol and variables with a standard deviation below 0.05. After this pretreatment the data set still contained thousands of variables. Subsequently, the SRD procedure was used to carry out the variable selection on groups of variables chosen according to their positions in 3-D space. Within the SRD procedure 400 seeds, a critical distance cutoff of 1.0 Å and a collapsing distance cutoff of 2.0 Å were used. The regions calculated were then used in a FFD variable selection procedure.

Model validation

To form the basis for a statistical significant model, the method of partial least squares (PLS) regression was used to analyze the 30 compounds by correlating variations in their biological activities with variations in their interacti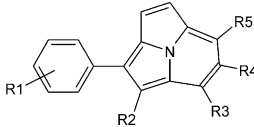on fields. The optimum number of PLS components corresponding to the smallest standard error of prediction, was determined by the leave-one-out (LOO) cross-validation procedure. Using the optimal number of components, the final PLS analysis was carried out without cross-validation to generate a predictive model with a conventional correlation coefficient. The LOO cross-validation method might lead to high q^2 values, which do not necessarily reflect a general predictiveness of a model. Therefore a second cross-validation, using five groups of approximately the same size in which the objects were assigned randomly, was performed. In this method 80% of the compounds were randomly selected and a model is generated, which is then used to predict the remaining compounds (leave-20%-out). This cross-validation technique has been shown to yield better indices for the robustness of a model than the normal LOO procedure.[56] The validated 3-D QSAR models obtained using different alignment strategies were then used for the prediction of the test set compounds. The quality of the external prediction is documented using the standard deviation of error prediction (SDEP).

Table 4. Observed and predicted estrogen receptor binding affinity (RBA) of pyrrolo[2,1,5-*cd*]-indolizines (test set 2)

Compd	R_1	R_2	R_3	R_4	R_5	$logRBA_{exp}$
6a	H	Et	H	OH	H	−1.27
6b	H	Et	H	H	OH	−0.41
6c	*p*-OH	Et	H	H	H	0.87
6d	*m*-OH	Et	H	H	H	−0.72
6e	*p*-OH	Et	CH_2OH	H	H	0.77
6f	*p*-OH	Et	H	H	OH	1.89
6g	*p*-OH	Et	H	OH	H	1.89
6h	*p*-OH	H	H	H	H	−1.00
6i	*p*-OH	Mel	H	H	H	0.40
6j	*p*-OH	*n*-Propyl	H	H	H	1.15
6k	*p*-OH	*i*-Propyl	H	H	H	0.94
6l	*p*-OH	$-(CH_2)_3-$		H	H	0.37
6m	*p*-OH	$-(CH_2)_4-$		H	H	0.45
6n	*p*-OH	*n*-Butyl	H	H	H	1.15

Table 5. Observed and predicted estrogen receptor binding affinity (RBA) of THC ligands (test set 3)

Compd	Stereochemistry	R	$logRBA_{exp}$
2	—	H	0.47
3	*trans*	Me	2.35
4	*cis*-(R,R)	Me	1.38
5	*cis*-(S,S)	Me	0.97
6	*trans*	Et	2.34
8	*cis*-(R,R)	Et	1.36
9	*cis*-(S,S)	Et	−0.04
10	*trans*	Pr	1.53
11	*cis*-(R,R)	Pr	0.72
12	*cis*-(S,S)	Pr	0.20

Interaction energy-based prediction

For the purpose of comparison, an alternative method was selected to predict the biological activities of the ER ligands. For this reason the binding energy of each ligand was retrieved from the receptor ligand complexes optimized with the YETI force field. Others and we found that the used parameters within YETI yield reliable results, which are in good agreement with experimental data.[36,43] Correlation between binding affinities and interaction energies were investigated by variation of several parameters during the geometry optimization and interaction energy evaluation phase. The best result was obtained by using AM1-ESP charges, a distance dependent dielectric constant ($\varepsilon = 2r$) and including receptor flexibility during the geometry optimization (for a detailed description of the method, see ref 39). The equation derived was then applied for the prediction of the test set molecules using the same parameters.

Results and Discussion

Docking simulations

All investigated ER ligands occupy a deeply buried, largely hydrophobic cavity. In the X-ray structures, estradiol and diethylstilbestrol bind in similar way to the receptor (Fig. 1). One of the phenolic rings of diethylstilbestrol lies in the same position as the aromatic ring of estradiol. Both ligands form hydrogen bonds to the γ-carboxylate of Glu353, to the guanidinium of Arg394 and to the imidazole ring of His524. In addition, the ligands show Van-der-Waals interactions with several hydrophobic residues in the binding pocket. The second hydroxyl group of diethylstilbestrol is located 1.7 Å from the position of the corresponding group of estradiol, but is still able to form a hydrogen bond to the imidazole ring of His524. The ethyl group of diesthylstilbestrol, which projects perpendicularly from the plane of the aromatic systems, fits into an additional cavity formed by several hydrophobic amino acid residues. The only major conformational difference between both receptor–agonist complexes is the orientation of the side chains of His524 and Met421. Due to the different size of diethylstilbestrol and estradiol, these side chains adopt different packing orientations in response to each ligand.

The docking simulations were started using the two molecules, estradiol and diethylstilbestrol, for which the binding mode has been experimentally determined. These two ligands were taken as positive control to test the docking program. AutoDock was successful in reproducing the experimentally found binding position. However, the crystal structure conformation of diethylstilbestrol was ranked by AutoDock only on position 3. After reranking the AutoDock results the crystal structure conformation was top-ranked. The RMSD values (all heavy atoms) between the observed and calculated position are 0.21 Å for estradiol and 0.37 Å for diethylstilbestrol. The ability to accurately predict the binding

conformations of estradiol and diethylstilbestrol gave confidence that we could use our model to evaluate the binding conformation of the remaining compounds for which no experimental data was available.

Receptor-based 3-D QSAR model

The superimposition of the ligands derived from the molecular docking was taken as starting point for a comparative molecular field analysis using the strategy described in the methods section. The top-ranked conformation for each ligand within the YETI force field was selected for the alignment generation. The optimization process applying the YETI force field changed the AutoDock ranking for most of the ligands. A detailed discussion of these findings can be found in a previous publication.[39] The resulting pharmacophore, which is shown in Figure 2a, is in agreement with other published models for estrogen receptor ligands.[4,57,58] The optimal number of latent variables was chosen by monitoring the changes in the fitting (r^2) and predictivity (q^2) indexes of the model upon adding a new latent variable. The maximum quality was obtained for a model with four latent variables. The statistical analysis yielded a correlation coefficient with a cross-validated q^2_{LOO} of 0.921 with a standard error of prediction (SDEP) of 0.345. The conventional r^2 of this analysis is 0.992 with a standard error of calculation (SDEC) of 0.112. This means, the model explains approximately 99% of the variance in ligand binding of the investigated compounds. The model is also robust, indicated by a high correlation coefficient of $q^2 = 0.900$ obtained by using the leave-20%-out cross-validation procedure.

Validation of the 3-D QSAR model

Besides the ligands used for the generation of the 3-D QSAR model other natural and synthetic compounds have been described in the literature, which also bind at the ER.[59,60] In order to test the predictivity of our model, a test set of six structurally diverse ER ligands was selected (Table 3). Using the described AutoDock/Yeti procedure, the molecules were docked into the binding pocket and the minimized conformations were used for the prediction of the binding affinity. The resulting molecular alignment is shown in Figure 3a. A standard error of prediction of 0.43 was obtained using the four-component model. The reasonable agreement between the predicted and observed RBA's substantiates the fitness of the GRID/GOLPE mode beyond the training set compounds.

Further support for our strategy came from the recently solved crystal structure of the ER complexed with genistein.[31] Since genistein was used in the external test set, it was interesting to see how well the experimentally observed complex agrees with the predicted one. In the crystal structure of the ER beta isoform (which is very similar to the previously reported alpha isoform) genistein is completely buried within the hydrophobic binding pocket and binds in a manner similar to that observed for estrogen and diethylstilbestrol. Figure 4 shows the superimposition of the predicted and experimentally determined complex, overlaid on their backbone atoms. The AutoDock/YETI procedure predicted correctly the orientation and conformation of genistein observed in the X-ray structure. The RMS deviation between the observed and predicted position is 0.75 (all
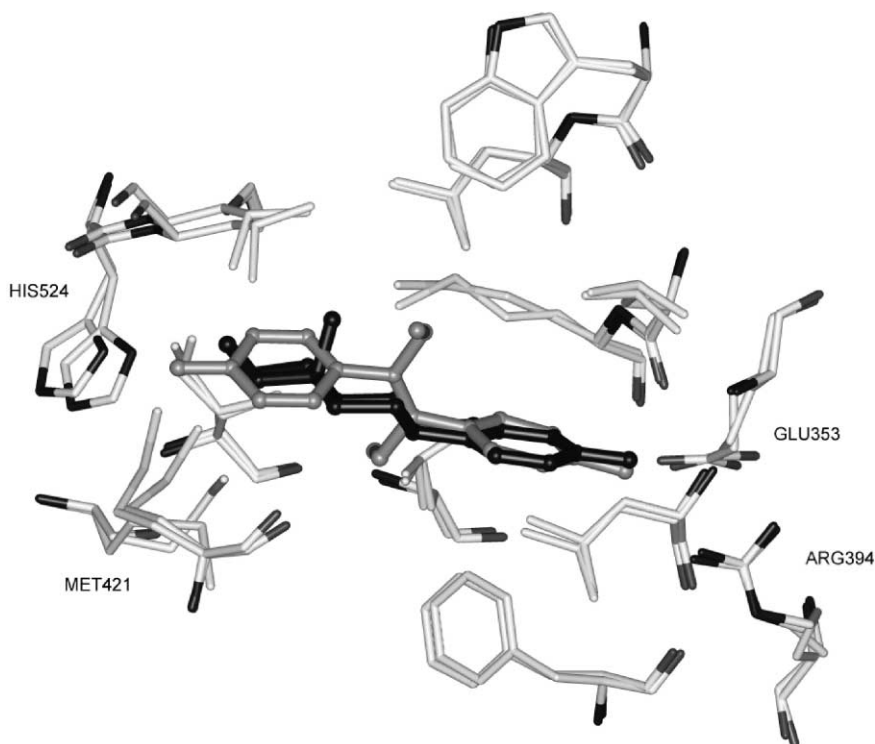

Figure 1. Comparison of the X-ray structures of the estrogen receptor liganded with estradiol (black) and diethylstilbestrol (grey). The two crystal structures were overlaid using the back-bone atoms. Only the amino acid residues in proximity to the binding pocket are shown for clarity.
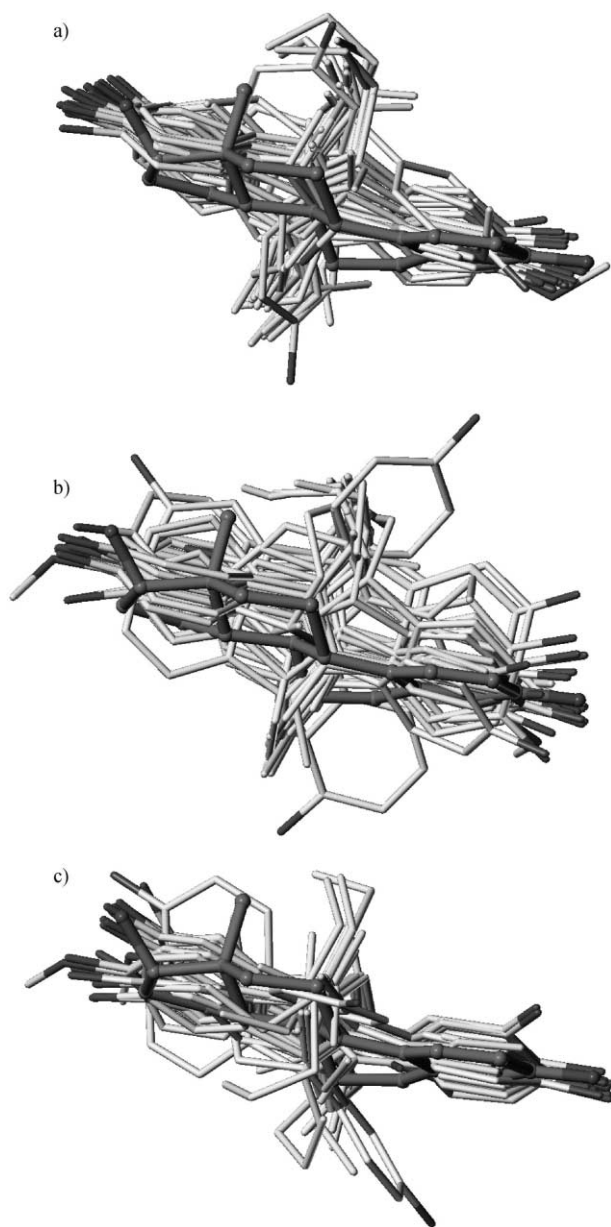
Figure 2. Alignment of 30 estrogen receptor ligands used for the model generation; (a) receptor-based alignment; (b) ligand-based alignment A; and (c) ligand-based alignment B (estradiol is colored dark grey).

Figure 3. Alignment obtained for the compounds of test set 1: (a) receptor-based alignment; (b) ligand-based alignment A; and (c) ligand-based alignment B (estradiol is colored dark grey).
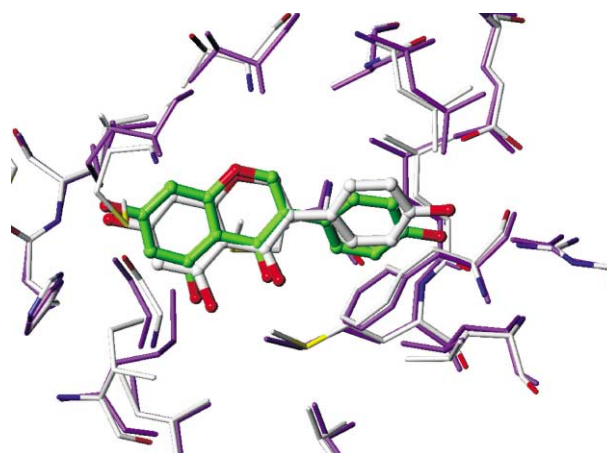
Figure 4. Comparison between predicted and X-ray structure of the estrogen receptor–genistein complex. The predicted structure of genistein and the estrogen receptor is colored green and violet, respectively, whereas the X-ray structure is colored by atom-type.

heavy atoms). On the basis of the docked genistein molecule a binding affinity of 0.66 was predicted compared to the experimentally determined affinity of 0.70.

Binding affinity prediction

The developed and validated 3-D QSAR model was subsequently used for the binding affinity prediction of several sets of ER ligands, which have been reported very recently.[8–11] Test set 2 (Table 4) comprises a series of 14 pyrrolo[2,1,5-*cd*]indolizine derivatives, which have been developed by Wassermann et al.[11] The parent compound **6a** was systematically modified to elucidate important features for affinity. Introduction of hydroxy groups in the pyrrolizidine and phenyl ring and variation of the alkyl-substituents improved the affinities. The most potent compounds **6f** and **6g** show sub-nanomolar affinities for the ER.

Test set 3 (Table 5) consists of a series of tetrahydrochrysene derivatives (THC) from Katzenellenbogen et al.[8] The variation of the alkyl-substituents as well

as the variation of the stereochemistry of the THC compounds were investigated. All molecules were separated and tested as pure stereoisomers, a prerequisite to the use of such compounds for QSAR analysis. The (S,S)-cis enantiomer series (**5**, **9** and **12**) shows only weak affinity at the ER, whereas the (R,R)-cis and the trans series possesses moderate to high affinity.

Test set 4 (Table 6) contains several hexaydrochrysene (HHC) and tetrahydrobenzo[a]fluorine derivatives (THBF) developed by Katzenellenbogen et al.[10] It is interesting to see that compounds with dissimilar molecular geometries (**12a** and **12b**) show comparably high affinity for the estrogen receptor.

All test set ligands were docked and scored as described in the methods section. For three compounds (**5**, **9**, **12**), AutoDock was not able to find any low energy conformation. A visual inspection of the binding site revealed that these compounds can only bind in a low energy conformation if several amino acids change their side-chain orientation. In the present version of Auto-Dock receptor flexibility can not be considered. For that reason the binding affinity for compound **5**, **9** and **12** could not be predicted. The remaining compounds were successfully docked by the AutoDock program. The ligand alignment as obtained by the docking procedure is displayed in Figures 5a, 6a and 7a. All molecules form a hydrogen bond to Glu353/Arg394 indicated by a similar position of the phenolic ring systems in the particular alignment. A second hydrogen bond to the imidazole of His524 is formed by the potent ligands. The derived alignment indicates further that the alkyl substituents of the ligands occupy similar regions in space corresponding to two hydrophobic cavities located on both sides of the planar ring systems of the co-crystallized ligands.

The conformations as obtained by the docking procedure were extracted from the binding site and were used for the prediction of binding affinity applying the developed GRID/GOLPE PLS model. The statistical results for all test set compounds are summarized in Tables 7–9. The external prediction yielded a predictive r_2 value of 0.656 [15] and a SDEP value of 0.531 for all test set compounds reflecting the good predictivity of the model. The average SDEP value of 0.531 for the
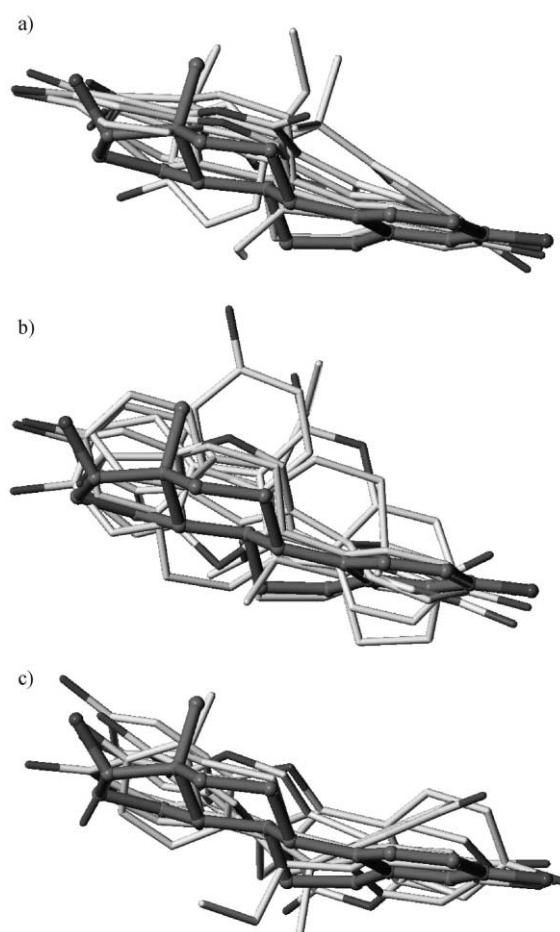

Figure 5. Alignment obtained for the compounds of test set 2: (a) receptor-based alignment; (b) ligand-based alignment A; and (c) ligand-based alignment B (estradiol is colored dark grey).

external prediction is, as expected, larger than for the internal validation (0.345), but sufficient to show the good predictivity of the model. In Figure 8a–d, the predicted logRBA values are plotted against experimental logRBA values for the individual test sets. The predictive r^2 and SDEP values derived for the individual test sets are listed in Tables 8 and 9, respectively. The SDEP values for the individual test sets are quite similar, not depending on the composition of the individual test sets. Larger deviations were observed for molecules possessing flexible substituents (**6j**, **6n** and **11**). The flexibility of the substituents leads to energetically very similar conformations during the docking simulation. Thus, it is difficult to decide which conformation is the bioactive one and should be considered for the alignment generation. The larger deviation observed during the prediction of compound **13** can be explained by the structurally different THBF system. None of the training set molecules contains a corresponding ring system/ substitutent at that position.

The subsequent PLS analysis, using the energy fields as descriptors and the binding affinity as the dependent variable, can highlight the relative importance for affinity of certain types of interaction and certain regions around the compounds. Since the structure of the

Table 6. Observed and predicted estrogen receptor binding affinity (RBA) of HHC and THBF ligands (test set 4)

Compd	Series	R	logRBA$_{exp}$
12a	cis-HHC		1.04
12b	trans-HHC	—	1.14
13	THBF	—	−0.27
14	THBF	H	0.94
17a	THBF	Et	1.68
17b	THBF	Et	2.18

Figure 6. Alignment obtained for the compounds of test set 3: (a) receptor-based alignment; (b) ligand-based alignment A; and (c) ligand-based alignment B (estradiol is colored dark grey).
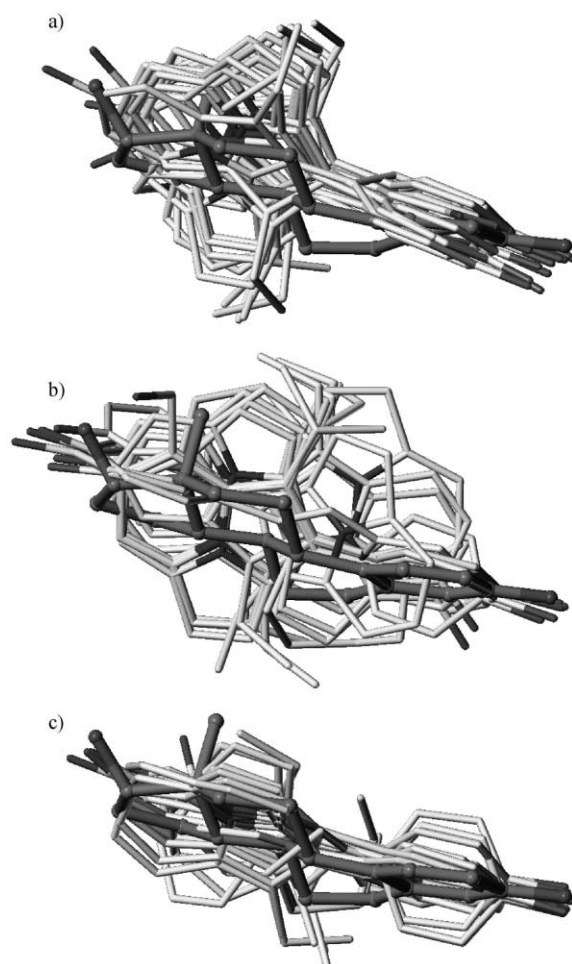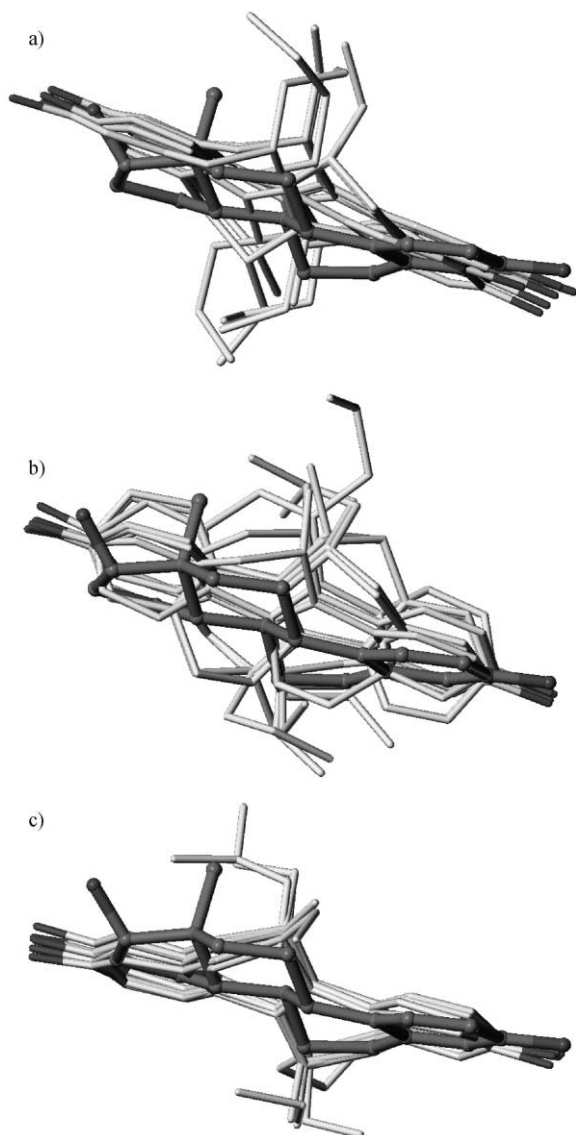

Figure 7. Alignment obtained for the compounds of test set 4: (a) receptor-based alignment; (b) ligand-based alignment A; and (c) ligand-based alignment B (estradiol is colored dark grey).

estrogen receptor is known, the results obtained by the 3-D QSAR analysis were compared with the geometry and properties of the binding pocket. It is necessary to note, that, in general, such comparison should be attempted carefully. The PLS coefficient contour maps can by no means be regarded as a set of low-resolution pictures of the binding site, since the contour maps reflect only those regions in space, where the ligand–probe interaction energy is correlated with a variance of the biological activity. However, it provides an opportunity to interpret features indicated in the contour maps with respect to the protein environment. We superimposed the coefficient contour maps and the active site of the estrogen receptor. Figures 9 and 10 show the grid plot of the PLS coefficients for the water probe. The contours in Figure 9 represent negative coefficients under −0.004 while the contours in Figure 10 represent positive coefficients over 0.004. Since we used the water probe the positive contour maps indicate

the areas where polar interaction decrease activity and the negative contour maps show the regions where polar interaction increase activity. In general, we observed an agreement between the maps and the positions of particular amino acid residues in the active site. For example, the positive-contoured field located in a hydrophobic pocket close to Leu346, Met421 and Ile424. The most active ligands of the four test sets possess alkyl substituents which are able to occupy this pocket. A second positive-contoured field coincides with Leu525, indicating that interactions between the aromatic ring system of the ligands and Leu525 influence ligand binding. The region around His524 and the backbone of Leu525 and Gly521 contains only negative coefficients indicating that polar interactions in that region would increase the activity. Less pronounced fields are located close to Glu353 and Arg394. Since most of the training set ligands possess a hydroxyl group which is able to interact with these two residues, it is not surprising that this region does not contribute to an explanation of the variation in the biological activities.

Interaction energy-based model

In the next step we focused on a possible correlation between the calculated protein–ligand interaction energy and the observed logRBA. The ligand–receptor interaction energy was calculated using the protocol described in the methods section. When trying to correlate the calculated interaction energies with the

Table 7. Observed and predicted estrogen receptor binding affinity (logRBA) for all compounds of the four external test sets

Compd	Observed	Receptor-based model	Ligand-based model A	Ligand-based model B	Interaction-energy model
Coumestrol	1.97	1.48	−0.02	0.43	−0.82
Genistein	0.70	0.66	0.39	1.08	1.14
Hexestrol	2.25	1.89	0.40	0.25	1.51
Bisphenol A	−1.30	−0.57	−0.01	0.81	−2.00
Estrone	1.78	1.46	−0.06	1.53	0.49
17α-Estradiol	1.76	1.55	1.38	1.05	0.76
6a	−1.27	−0.47	0.35	0.15	−0.05
6b	−0.41	−0.11	0.32	0.97	−0.24
6c	0.87	0.25	0.73	0.07	0.62
6d	−0.72	−0.01	0.01	−1.17	0.43
6e	0.77	1.18	0.46	1.55	−0.20
6f	1.89	1.89	−0.10	1.46	0.77
6g	1.89	2.73	0.95	0.91	1.29
6h	−1.00	−0.65	−0.23	0.73	0.14
6i	0.40	0.80	0.57	1.10	0.10
6j	1.15	0.34	0.72	0.49	0.03
6k	0.94	0.86	0.8	0.79	−0.15
6l	0.37	−0.22	0.47	0.87	−0.26
6m	0.45	−0.03	0.02	0.86	−0.55
6n	1.15	0.15	0.85	0.82	0.15
2	0.47	1.24	0.71	1.65	1.41
3	2.35	1.85	2.19	2.28	1.31
4	1.38	1.19	1.29	2.04	−0.28
6	2.34	1.80	2.57	2.56	1.77
8	1.36	1.60	1.45	1.96	−0.56
10	1.53	1.78	1.88	2.66	0.50
11	0.72	1.64	1.53	1.57	−0.66
12a	1.04	1.07	1.47	1.10	0.35
12b	1.14	1.18	0.62	1.42	−0.21
13	−0.27	0.99	0.14	0.35	0.73
14	0.94	0.89	−0.25	0.69	0.54
17a	1.68	1.21	0.01	1.04	1.02
17b	2.18	2.28	1.26	1.48	0.80

Table 8. Predictive r^2 values obtained for the different test sets

Test set	Receptor-based model	Ligand-based model A	Ligand-based model B	Interaction-energy model
Test set 1	0.778	−1.674	−0.550	−1.513
Test set 2 (Pyrrolo)	0.675	0.629	0.338	0.227
Test set 3 (THC)	0.595	0.823	0.195	−1.220
Test set 4 (THBF)	0.508	−0.531	0.615	−1.112
All test set molecules	0.656	0.003	0.203	−0.487

Table 9. External SDEP values obtained for the different test sets

Test set	Receptor-based model	Ligand-based model A	Ligand-based model B	Interaction-energy model
Test set 1	0.430	1.455	1.386	1.395
Test set 2 (Pyrrolo)	0.549	0.900	0.945	0.889
Test set 3 (THC)	0.555	0.366	0.780	1.294
Test set 4 (THBF)	0.552	0.972	0.486	0.982
All test set molecules	0.531	0.964	0.949	1.104

binding affinities, it turned out that the chosen protocol leads to a statistically significant correlation for the 30 training set molecules. The correlation coefficient r^2 for the 30 compounds is 0.617 ($q^2 = 0.570$), which is much lower as the one obtained with the 3-D QSAR model. However, we also used the interaction energy-based model for the prediction of the test set compounds.

The influence of the minimization protocol on the statistical results was already tested in a previous publication.[39] Only small differences in the predictivity of the models were observed. Therefore, only the protocol which yielded the most predictive model was applied for the prediction of the test set ligands. The analysis of the test set compounds shows that the interaction energy, as calculated with the AutoDock/YETI proce-

dure, cannot be used for the prediction of the ligand binding affinity. This is demonstrated by the low predictive r^2 value of -0.487. The average SDEP value for all test set compounds is 1.104 compared to 0.531 obtained for the 3-D QSAR model. The quality of the prediction is not depending on the composition of the individual test set (Table 7). We found that the most potent compounds (coumestrol, **6g**, **17b**) were underpredicted whereas the less active compounds (**6a**, **6h**, **6d**) were overpredicted.
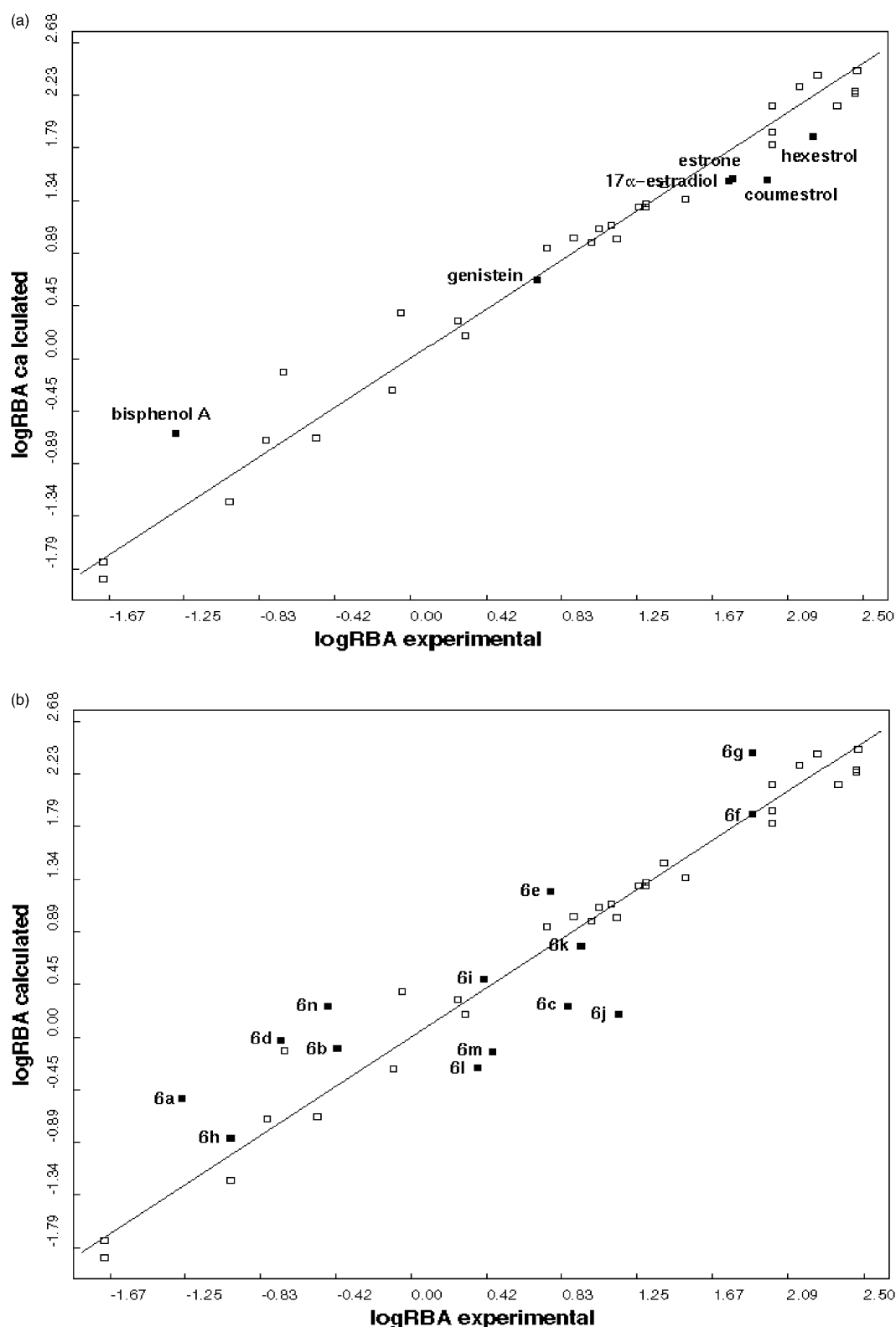

Figure 8. The figures show the statistical results for the prediction of the four external test sets obtained with the receptor-based GRID/GOLPE model: (a) test set 1, (b) test set 2 (c) test set 3, (d) test set 4.

3752

W. Sippl / Bioorg. Med. Chem. 10 (2002) 3741–3755
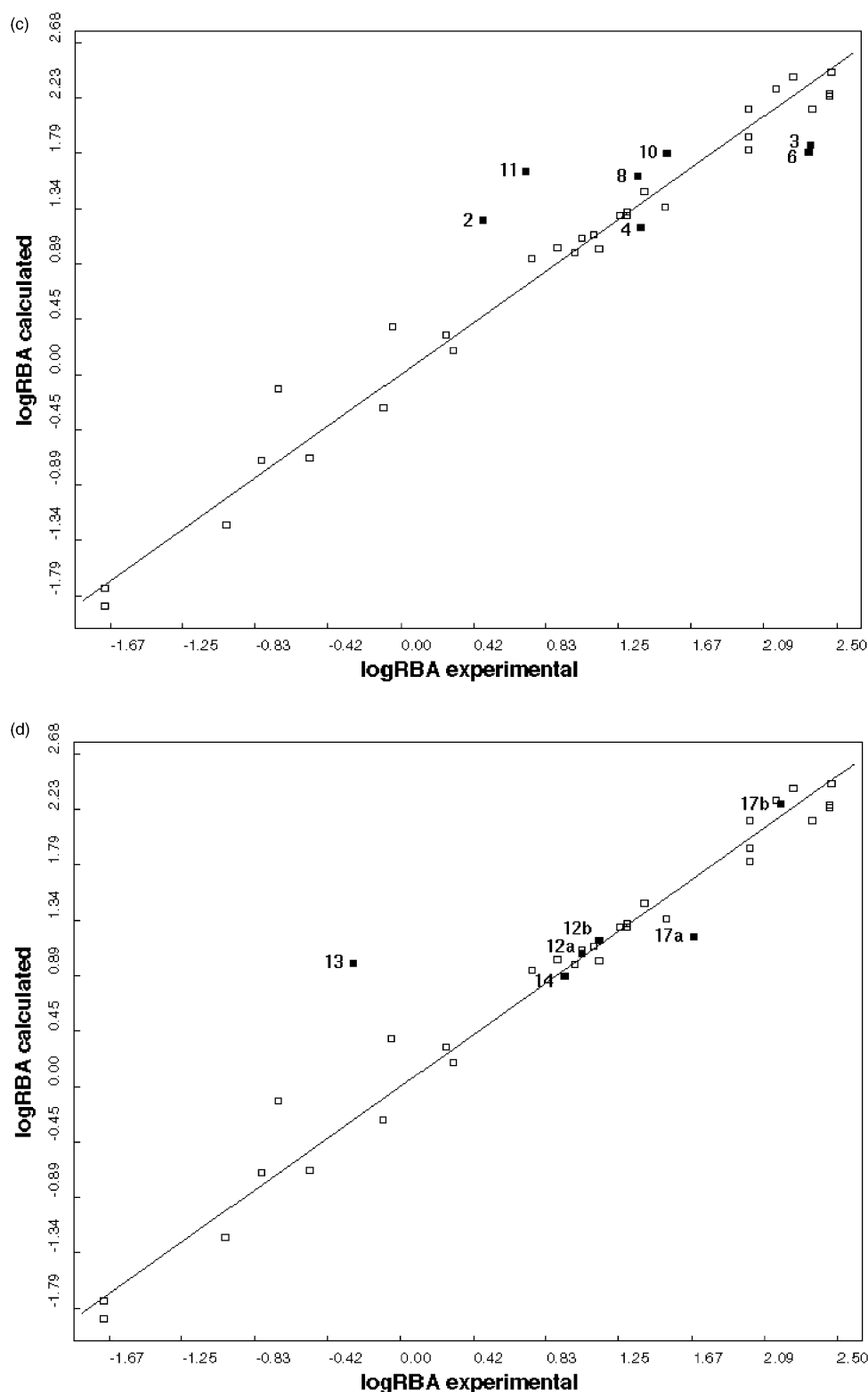
Figure 8. (*continued*)

It appeared relatively difficult to find a predictive model based on the calculated interaction energies. Several reasons for the low predictivity of interaction-energy based models have been stated in the literature.[62] Small errors in atomic coordinates which occur as well in well-refined X-ray structures have considerable influence on the energy landscape of ligand binding. To rank computer-generated ligands correctly the affinity estimation method must be able to correctly position novel ligands within the binding pocket and optimize their non-covalent interaction with the protein. The errors in this calculated positions are unlikely to be smaller than those of the coordinates of the protein atoms, so the estimation of affinity must be able to

Figure 9. Comparison between the PLS coefficient maps, contoured at −0.004, and the amino acid residues located close to the binding pocket. The region around His524 and the backbone of Leu525 and Gly521 contains only negative coefficients indicating that polar interactions here would increase the activity (diethylstilbestrol is colored dark grey, and the most potent training set ligand, compound **17**, is colored grey).
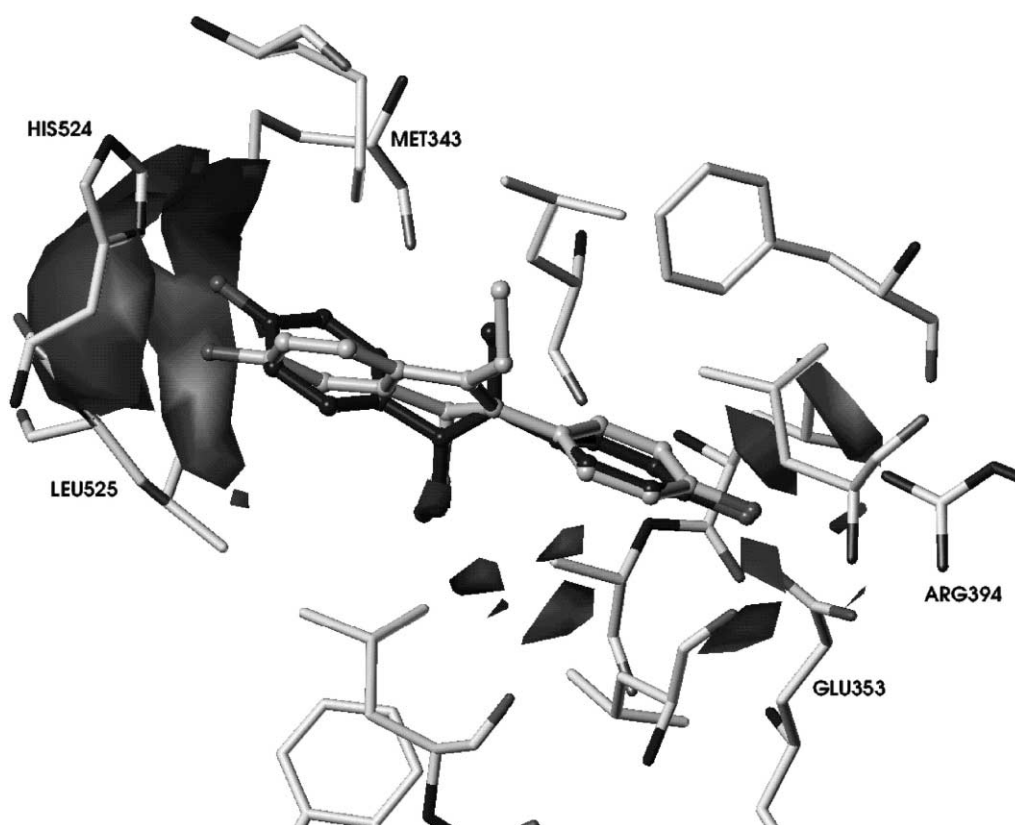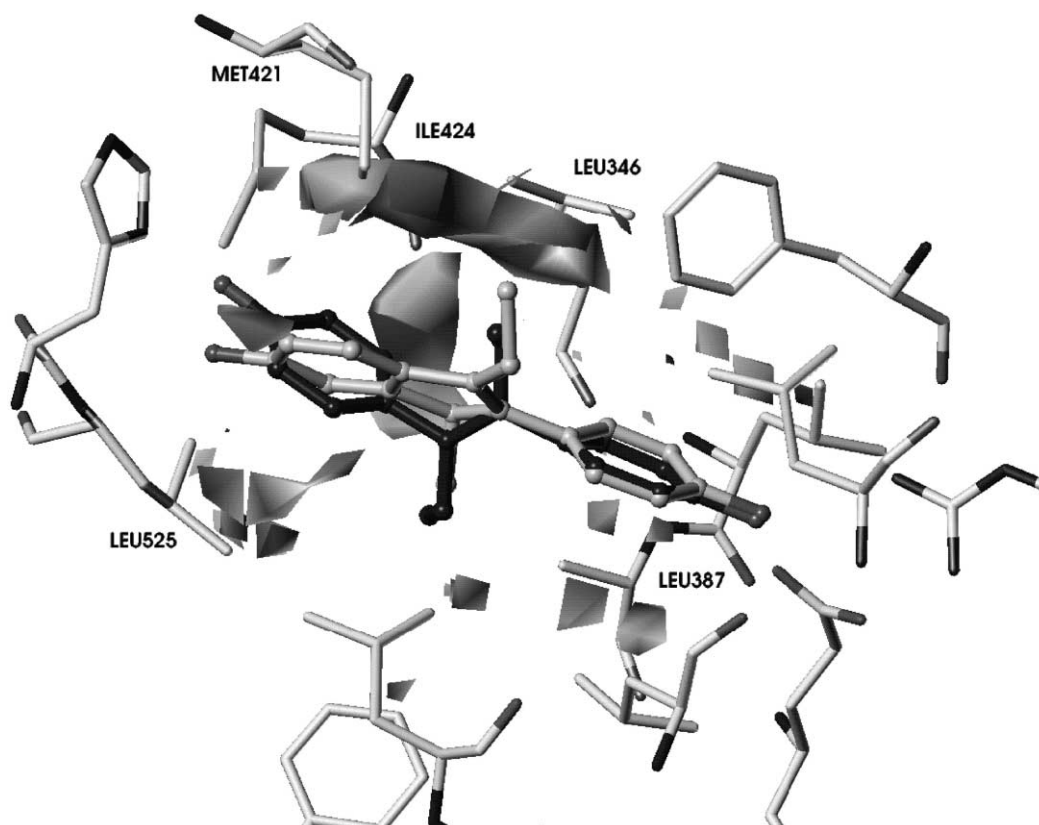

Figure 10. Comparison between the PLS coefficient maps, contoured at +0.004, and the amino acid residues located close to the binding pocket. (Diethylstilbestrol is colored dark grey, and the most potent training set ligand, compound **17**, is colored grey.

accommodate small deviation in atom positions. Another problem is the limited understanding of the physics and thermodynamics of ligand binding, especially solvation and entropic effects are at the moment fully neglected by interaction-energy based models. To overcome this problem more rigorous methods such as the free energy perturbation method have to be applied. For a detailed discussion of these problems, see refs 62–64.

Ligand-based 3-D QSAR models

The presented receptor-based approaches, either based on GRID/GOLPE PLS analysis or based on ligand–receptor interaction energies, require the three-dimensional structure of the target protein. However, this information is not available for a huge number of therapeutically interesting compounds. In this situation ligand-based alignment strategies are applied in order to deduce quantitative structure–activity relationships. In the present study the performance of two ligand-based alignment strategies was tested and compared with the receptor-based results. For that purpose we applied program FlexS, which superimposes flexible molecules onto a template structure.[30] Alignment A was obtained by fitting all training and test set compounds onto diethylstilbestrol (Figs 2b, 4b, 5b, 6b, and 7b). The coordinates of the diethylstilbestrol molecule were taken from the X-ray structure of the diethylstilbestrol–receptor complex. For the generation of alignment B estradiol was considered as template molecule (Figs 2c, 4c, 5c, 6c, and 7c). The hydroxyl groups, which are considered as strong hydrogen-bond donors/acceptors by FlexS, are perfectly superimposed in both ligand-based alignments. In the receptor-based alignment these groups show a broader variation, since the alignment is influenced by the geometry of the binding–pocket. Greater differences were observed in the positions of the bulky hydrophobic ring systems.

On the basis of the ligand-based alignments, GRID/GOLPE PLS analyses were carried out using the SRD/FFD procedure as described in the Methods section. As was the case in the GRID/GOLPE analysis of the receptor-based alignment, the optimal number of principal components was chosen by monitoring the changes in the predictive ability (q^2_{LOO}) index of the model upon addition of a new latent variable. The maximum quality was obtained for models with three principle components. In cross-validation the predictive ability of the resulting models were tested. Model A yielded the following statistical results: $r^2 = 0.923$, $q^2_{LOO} = 0.631$ and SDEP = 0.744, whereas the model based on alignment B shows better fitting and predictive indexes ($r^2 = 0.971$, $q^2_{LOO} = 0.851$ and SDEP = 0.463). The PLS models were subsequently used for the prediction of the 33 test set compounds. Both models show quite similar predictive r^2 and SDEP values (see Tables 8 and 9 for details). Compared to the receptor-based PLS model, the predictive ability of the ligand-based models is quite low. Both PLS models have problems to correctly predict the compounds included in test set 1. Since test set 1 consists of compounds structurally not related to the training set molecules, it is obvious why the ligand-based approaches fail to predict these compounds correctly.

Conclusions

In the present study, several 3-D QSAR methods have been applied to estimate the binding affinities of recently developed ER ligands. The combination of docking and 3-D QSAR methods yielded a model with good external predictivity. Two ligand-based alignments were additionally generated using the FlexS program. The ligand-based 3-D QSAR models are shown to have low predictive ability.

The generated receptor-based alignment reflects a mutual superposition of the ligands along with their relative orientation towards the binding pocket. In this way, information about the geometry of the binding pocket is included in the ligand alignment. Without using this information, the molecular interaction fields act only as general shape descriptors, but do not really represent the binding site.

The combined approach of docking studies and QSAR analysis allowed us to gain insight into the structural basis for estrogen receptor binding. From a methodological point of view, the applied procedure seems to be a generally sound methodology which allows one to merge the experimentally derived information from ligand–protein structures with the computational power of QSAR. In this particular case, the combination of AutoDock 3.0 and the YETI force field was shown to be able to reproduce the experimentally observed binding mode of estrogen receptor ligands.

In addition we analyzed whether using receptor–ligand interaction energies could serve as basis for a predictive model. The external predictivity of the derived model was quite low, indicating the problem of using interaction energies for ranking. The neglect of solvation or entropic terms is probably one reason of the poor performance or the interaction energy-based model. It is also clear that the used interaction energy-based approach is a relatively poor scoring method that only works to some extent for high-resolution structures. This finding confirms the continuous need in drug design projects for experimental verification of models by determining high-resolution structures of key compounds in complex with their receptor.[35,65,66]

We guess that a multivariate QSAR analysis is able to provide a kind of scoring function valid for a particular data set. This has been successfully demonstrated for the investigated estrogen receptor ligands. Sine the applied method is computationally not demanding it can be applied for the screening of large ligand series. As long as no methods are available which are able to solve the affinity prediction problem, receptor-based 3-D QSAR is an interesting strategy for drug design projects.

Acknowledgements

References and Notes

1. Evans, R. M. *Science* **1988**, *240*, 889.
2. Zeelen, F. J. *Medicinal Chemistry of Steroids*; Elsevier: Amsterdam, 1990.
3. Von Angerer, E. *The Estrogen Receptor as a Target for Rational Drug Design*; Landes: Austin, USA, 1995.
4. Anstead, G. M.; Carlson, K. E.; Katzenellenbogen, J. A. *Steroids* **1996**, *62*, 268.
5. Inestrosa, N. C.; Marzolo, M. P.; Bonnefont, A. B. *Mol. Neurobiol.* **1998**, *17*, 73.
6. Bhat, R. A.; Harnish, D. C.; Stevis, P. E.; Lyttle, C. R.; Komm, B. S. *J. Steroid. Biochem. Mol. Biol.* **1998**, *67*, 233.
7. Brzozowski, A. M.; Pike, A. C.; Dauter, Z.; Hubbard, R. E.; Bonn, T.; Engstrom, O.; Ohman, L.; Greene, G. L.; Gustafsson, J. A.; Carlquist, M. *Nature* **1997**, *389*, 753.
8. Meyers, M. J.; Sun, J.; Carson, K. E.; Katzenellenbogen, B. S.; Katzenellenbogen, J. A. *J. Med. Chem.* **1999**, *42*, 2456.
9. Stauffer, S. R.; Huang, Y.; Coletta, C. J.; Tedesco, R.; Katzenell enbogen, J. A. *Bioorg. Med. Chem.* **2000**, *9*, 141.
10. Tedesco, R.; Youngman, M. K.; Wilson, S. R.; Katzen-ellenbogen, J. A. *Bioorg. Med. Chem. Lett.* **2001**, *11*, 1281.
11. Jorgensen, A. S.; Jacobsen, P.; Christiansen, L. B.; Bury, P. S.; Kanstrup, A.; Thorpe, S. M.; Naerum, L.; Wassermann, K. *Bioorg. Med. Chem. Lett.* **2000**, *10*, 2383.
12. Gust, R.; Keititz, R.; Schmidt, K. *J. Med. Chem.* **2001**, *44*, 1963.
13. Hansch, C.; Leo, A. *Exploring QSAR. Fundamentals and applications in Chemistry and Biology*; American Chemical Society: Columbus, USA, 1995.
14. Kubinyi, H. *Drug Discov. Today* **1997**, *2*, 457.
15. Cramer, R. D.III; Patterson, D. E.; Bunce, J. D. *J. Am. Chem. Soc.* **1988**, *110*, 5959.
16. Kubinyi, H., Ed., *3-D QSAR in Drug Design. Theory, Methods and Applications*. ESCOM Science. Leiden, 1993
17. Kuntz, J. D. *Science* **1992**, *257*, 1078.
18. Kim, K. J. *Comput. Aided Mol. Des.* **1993**, *7*, 71.
19. Folkers, G., Merz, A.; Rognan, D. In *3-D QSAR in Drug Design. Theory, Methods and Applications*; Kubinyi, H., Ed.; ESCOM Science: Leiden, 1993; p 583.
20. Klebe, G.; Abraham, U. *J. Med. Chem.* **1993**, *36*, 70.
21. Viswanadhan, V. N.; Reddy, M. R.; Wlodawer, A.; Var-ney, M. D.; Weinstein, J. *J. Med. Chem.* **1996**, *39*, 705.
22. Kramer, B.; Rarey, M.; Lengauer, T. *Proteins (Suppl. 1)* **1997**, 221.
23. Morris, G. M.; Goodsell, D. S.; Huey, R.; Olson, A. J. *J. Comput. Aided Mol. Des.* **1994**, *8*, 243.
24. Lybrand, T. P. *Curr. Opin. Struct. Biol.* **1995**, *5*, 224.
25. Meng, E.; Shoichet, B. K.; Kuntz, I. D. *J. Comput. Chem.* **1992**, *13*, 505.
26. Tame, J. R. H. *J. Comput. Aided Mol. Des.* **1999**, *13*, 99.
27. Böhm, H. J. *J. Comput. Aided Mol. Des.* **1998**, *12*, 309.
28. Böhm, H. J. *J. Comput. Aided Mol. Des.* **1994**, *8*, 243.
29. Wang, R.; Liu, L.; Lai, L.; Tang, Y. *J. Mol. Model.* **1998**, *4*, 379.
30. Lemmen, C.; Lengauer, T.; Klebe, G. *J. Med. Chem.* **1998**, *41*, 4502.
31. Oostenbrink, B. C.; Pitera, J. W.; van Lipzig, M. M. H.; Meerman, J. H. N.; van Gunsteren, W. F. *J. Med. Chem.* **2000**, *43*, 4594.
32. Waller, C. L.; Oprea, T. I.; Giolitti, A.; Marshall, G. R. *J. Med. Chem.* **1993**, *36*, 4152.
33. De Priest, S. A.; Mayer, D.; Naylor, C. B.; Marshall, G. R. *J. Am. Chem. Soc.* **1993**, *115*, 5372.
34. Cho, S. J.; Garsia, M. L.; Bier, J.; Tropsha, A. *J. Med. Chem.* **1996**, *39*, 5064.
35. Vaz, R. J.; McLean, L. R.; Pelton, J. T. *J. Comput. Aided Mol. Des.* **1998**, *12*, 99.
36. Sippl, W.; Contreras, J. M.; Parrot, I.; Rival, Y.; Wer-muth, C.G. *J. Comput. Aided Mol. Des* **2001**, *15*, 395.
37. Afzelius, L.; Zamora, I.; Ridderström, M.; Andersson, T. B.; Karlen, A.; Masimirembwa, C. M. *Mol. Pharmacol.* **2001**, *59*, 909.
38. Sadler, B. R.; Cho, S. J.; Ishaq, K. S.; Chae, K.; Korach, K. S. *J. Med. Chem.* **1998**, *41*, 2261.
39. Sippl, W. *J. Comput. Aided Mol. Des.* **2000**, *14*, 559.
40. Bernstein, F. C.; Koetzle, T. F.; Williams, G. J. B.; Meyer, E. F.; Brice, M. D.; Rodgers, J. R.; Kennard, O.; Shima-nouchi, T.; Tasumi, M. *J. Mol. Biol.* **1997**, *112*, 535.
41. Weiner, S. J.; Kollman, P. A.; Case, D. A.; Singh, U. C.; Ghio, C.; Alagona, G.; Profeta, S.; Weiner, P. J. *J. Am. Chem. Soc.* **1984**, *106*, 765.
42. Singh, U. C.; Kollman, P. A. *J. Comput. Chem.* **1984**, *5*, 129.
43. Vedani, A.; Huhta, D. W. *J. Am. Chem. Soc.* **1990**, *112*, 269.
44. Goodsell, D. S.; Morris, G. M.; Olson, A. J. *J. Mol. Recognit.* **1996**, *9*, 1.
45. Rao, M. J.; Olson, A. J. *Prot. Struct. Funct. Gen.* **1999**, *34*, 173.
46. Goodford, P. J. *J. Med. Chem.* **1985**, *28*, 849.
47. Vedani, A.; Dunitz, J. D. *J. Am. Chem. Soc.* **1985**, *107*, 7653.
48. *PrGen 1.5.6*; Biographics Laboratory; Basel, Switzerland.
49. *GRID 16*; Molecular Discovery Ltd.; Oxford, UK.
50. *GOLPE 4.0*; Multivariate Infometric Analysis, Perugia, Italy.
51. Baroni, M.; Constantino, G.; Cruciani, G.; Riganelli, D; Valigli, R.; Clementi, S. *Quant. Struct.-Act. Relat.* **1993**, *12*, 9.
52. *SYBYL 6.5*, Tripos Inc.: St. Louis, MO, USA.
53. Cruciani, G.; Watson, K. *J. Med. Chem.* **1994**, *37*, 2589.
54. Pastor, M.; Cruciani, G.; Watson, K. *J. Med. Chem.* **1997**, *40*, 4089.
55. Pastor, M.; Cruciani, G.; Clementi, S. *J. Med. Chem.* **1997**, *40*, 1455.
56. Oprea, T. I.; Garcia, A. E. *J. Comput. Aided Mol. Des.* **1996**, *10*, 186.
57. Lewis, D. F. V.; Parker, M. G.; King, R. J. B. *J. Steroid. Biochem. Mol. Biol.* **1995**, *52*, 55.
58. Goldstein, R. A.; Katzenellenbogen, J. A.; Luthey-Schul-ten, Z. A.; Seielstad, D. A.; Wolynes, P. G. *Proc. Natl. Acad. Sci. U.S.A.* **1993**, *90*, 9949.
59. Tong, W.; Perkins, R.; Xing, L.; Welsh, W. J.; Sheehan, D. M. *Endocrinology* **1997**, *138*, 4022.
60. Waller, C. L.; Oprea, T. I.; Chae, K.; Park, H. K.; Kor-ach, K. S.; Laws, S. C.; Wiese, T. E.; Kelce, W. R.; Gray, L. E. *Chem. Res. Toxicol.* **1996**, *9*, 1240.
61. Pike, A. C. W.; Brzozowski, A. M.; Hubbard, R. E.; Bonn, T.; Thorsell, A. G.; Engström, O.; Ljunggren, J.; Gus-tafsson, J. A.; Carlquist, M. *EMBO* **1999**, *18*, 4608.
62. Tame, J. R. H. *J. Comput. Aided Mol. Des.* **1999**, *13*, 99.
63. Donini, O. A.; Kollman, P. A. *J. Med. Chem.* **2000**, *43*, 4180.
64. Aqvist, J.; Marelius, J. *Comb. Chem. High Throughput Screen.* **2001**, *4*, 613.
65. Bursi, R.; Grootenhuis, P. D. *J. Comput. Aided Mol. Des.* **1999**, *13*, 221.
66. So, S. S.; Karplus, M. *J. Comput. Aided Mol. Des.* **1999**, *13*, 243.